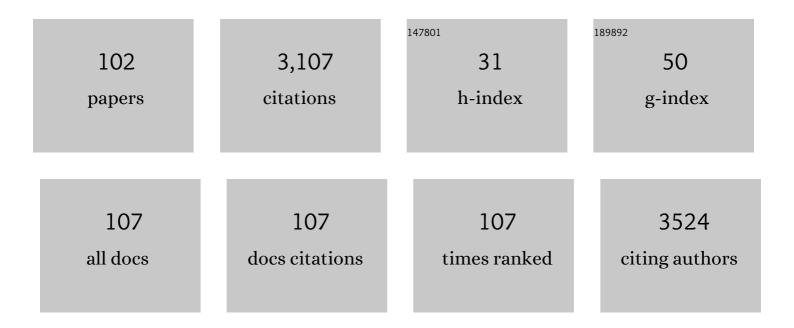
Liping Wang

List of Publications by Year in descending order

Source: https://exaly.com/author-pdf/5332978/publications.pdf Version: 2024-02-01



#	Article	IF	CITATIONS
1	A New Molybdenum Nitride Catalyst with Rhombohedral MoS ₂ Structure for Hydrogenation Applications. Journal of the American Chemical Society, 2015, 137, 4815-4822.	13.7	195
2	New calibration of infrared measurement of dissolved water in rhyolitic glasses. Geochimica Et Cosmochimica Acta, 1997, 61, 3089-3100.	3.9	147
3	Thermal equations of state of thel 2 , andl $^\infty$ phases of zirconium. Physical Review B, 2005, 71, .	3.2	113
4	Diffusion of the hydrous component in pyrope. American Mineralogist, 1996, 81, 706-718.	1.9	105
5	Plastic deformation of silicon between 20 °C and 425 °C. Physica Status Solidi C: Current Topics in Solid State Physics, 2007, 4, 3110-3114.	0.8	104
6	Soft and Selfâ€Adhesive Thermal Interface Materials Based on Vertically Aligned, Covalently Bonded Graphene Nanowalls for Efficient Microelectronic Cooling. Advanced Functional Materials, 2021, 31, 2104062.	14.9	95
7	Reaction mechanism studies towards effective fabrication of lithium-rich anti-perovskites Li3OX (X=) Tj ETQq1	1 0.784314 2.7	rgBT /Overlo
8	Mineral inclusions in pyrope crystals from Garnet Ridge, Arizona, USA: implications for processes in the upper mantle. Contributions To Mineralogy and Petrology, 1999, 135, 164-178.	3.1	85
9	Experimental constraints on the phase diagram of elemental zirconium. Journal of Physics and Chemistry of Solids, 2005, 66, 1213-1219.	4.0	77
10	Weakening of calcium iridate during its transformation from perovskite to post-perovskite. Nature Geoscience, 2009, 2, 794-797.	12.9	74
11	In Situ XRD Studies of ZnO/GaN Mixtures at High Pressure and High Temperature: Synthesis of Zn-Rich (Ga _{1â^'<i>x</i>} Zn _{<i>x</i>})(N _{1â^'<i>x</i>} O _{<i>x</i>}) Photocatalysts. Journal of Physical Chemistry C, 2010, 114, 1809-1814.	3.1	71
12	Elasticity of polycrystalline pyrope (Mg3Al2Si3O12) to 9GPa and 1000°C. Physics of the Earth and Planetary Interiors, 2006, 155, 179-190.	1.9	68
13	Vanadium Diboride (VB ₂) Synthesized at High Pressure: Elastic, Mechanical, Electronic, and Magnetic Properties and Thermal Stability. Inorganic Chemistry, 2018, 57, 1096-1105.	4.0	64
14	New measurements of activation volume in olivine under anhydrous conditions. Physics of the Earth and Planetary Interiors, 2009, 172, 67-73.	1.9	62
15	In situx-ray diffraction study of silicon at pressures up to 15.5 GPa and temperatures up to 1073 K. Physical Review B, 2003, 68, .	3.2	61
16	Synthesis, Hardness, and Electronic Properties of Stoichiometric VN and CrN. Crystal Growth and Design, 2016, 16, 351-358.	3.0	50
17	Crystal structures, elastic properties, and hardness of high-pressure synthesized CrB2 and CrB4. Journal of Superhard Materials, 2014, 36, 279-287.	1.2	49
18	Enhanced ionic conductivity with Li7O2Br3 phase in Li3OBr anti-perovskite solid electrolyte. Applied Physics Letters, 2016, 109, .	3.3	48

#	Article	IF	CITATIONS
19	Thermal equations of state for titanium obtained by high pressure—temperature diffraction studies. Physical Review B, 2008, 78, .	3.2	47
20	Experimental invalidation of phase-transition-induced elastic softening in CrN. Physical Review B, 2012, 86, .	3.2	47
21	Network Rigidity in <mml:math <br="" xmlns:mml="http://www.w3.org/1998/Math/MathML">display="inline"><mml:msub><mml:mi>GeSe</mml:mi><mml:mn>2</mml:mn></mml:msub></mml:math> Glass at High Pressure. Physical Review Letters, 2008, 100, 115501.	7.8	46
22	Precise stress measurements with white synchrotron x rays. Review of Scientific Instruments, 2010, 81, 013903.	1.3	42
23	Fe-Mg order-disorder in orthopyroxenes. Geochimica Et Cosmochimica Acta, 2005, 69, 5777-5788.	3.9	40
24	Pressure-Induced Amorphization and Phase Transformations in Î ² -LiAlSiO4. Chemistry of Materials, 2005, 17, 2817-2824.	6.7	37
25	Simultaneous ultrasonic and synchrotron x-ray studies on pressure induced α-ω phase transition in zirconium. Journal of Applied Physics, 2008, 104, .	2.5	36
26	Thermal equation of state of rhenium diboride by high pressure-temperature synchrotron x-ray studies. Physical Review B, 2008, 78, .	3.2	35
27	Pressure-induced structural and electronic transitions, metallization, and enhanced visible-light responsiveness in layered rhenium disulphide. Physical Review B, 2018, 97, .	3.2	35
28	Elasticity of <mml:math <br="" xmlns:mml="http://www.w3.org/1998/Math/MathML">display="inline"><mml:mi>ω</mml:mi></mml:math> -phase zirconium. Physical Review B, 2007, 76, .	3.2	34
29	Do Reuss and Voigt bounds really bound in high-pressure rheology experiments?. Journal of Physics Condensed Matter, 2006, 18, S1049-S1059.	1.8	33
30	Thermomechanics of Nanocrystalline Nickel under High Pressureâ^'Temperature Conditions. Nano Letters, 2007, 7, 426-432.	9.1	33
31	High pressure-high temperature synthesis of lithium-rich Li3O(Cl, Br) and Li3â^'xCax/2OCl anti-perovskite halides. Inorganic Chemistry Communication, 2014, 48, 140-143.	3.9	33
32	Thermal equation of state of silicon carbide. Applied Physics Letters, 2016, 108, .	3.3	33
33	Elasticity and sound velocities of polycrystalline grossular garnet (Ca3Al2Si3O12) at simultaneous high pressures and high temperatures. Physics of the Earth and Planetary Interiors, 2014, 228, 80-87.	1.9	31
34	Deformation of olivine at subduction zone conditions determined from in situ measurements with synchrotron radiation. Physics of the Earth and Planetary Interiors, 2011, 186, 23-35.	1.9	30
35	The strength of moissanite. American Mineralogist, 2002, 87, 1005-1008.	1.9	29
36	Constitutive Law and Flow Mechanism in Diamond Deformation. Scientific Reports, 2012, 2, 876.	3.3	29

#	Article	IF	CITATIONS
37	Synthesis of Onion-Like δ-MoN Catalyst for Selective Hydrogenation. Journal of Physical Chemistry C, 2017, 121, 19451-19460.	3.1	29
38	Structural Studies of the Natural Antimonian Pyrochlores. Journal of Solid State Chemistry, 1998, 141, 562-569.	2.9	28
39	In situ X-ray diffraction study of germanium at pressures up to 11 GPa and temperatures up to 950K. Journal of Physics and Chemistry of Solids, 2003, 64, 2113-2119.	4.0	28
40	Diamond- <i>c</i> BN alloy: A universal cutting material. Applied Physics Letters, 2015, 107, .	3.3	28
41	Experimental constraints on the phase diagram of titanium metal. Journal of Physics and Chemistry of Solids, 2008, 69, 2559-2563.	4.0	27
42	Synthesis and Structure of Perovskite ScMnO ₃ . Inorganic Chemistry, 2013, 52, 9692-9697.	4.0	27
43	Phase-Transition Induced Elastic Softening and Band Gap Transition in Semiconducting PbS at High Pressure. Inorganic Chemistry, 2013, 52, 8638-8643.	4.0	27
44	The elastic properties of β-Mg2SiO4 from 295 to 660K and implications on the composition of Earth's upper mantle. Physics of the Earth and Planetary Interiors, 2007, 162, 22-31.	1.9	26
45	Sulfur-catalyzed phase transition in MoS2 under high pressure and temperature. Journal of Physics and Chemistry of Solids, 2014, 75, 100-104.	4.0	26
46	Pressure and temperature dependence of the elasticity of pyrope–majorite [Py60Mj40 and Py50Mj50] garnets solid solution measured by ultrasonic interferometry technique. Physics of the Earth and Planetary Interiors, 2009, 174, 105-112.	1.9	25
47	Thermal equation of state of copper studied by high P-T synchrotron x-ray diffraction. Applied Physics Letters, 2009, 94, .	3.3	25
48	Revisit of Pressure-Induced Phase Transition in PbSe: Crystal Structure, and Thermoelastic and Electrical Properties. Inorganic Chemistry, 2015, 54, 4981-4989.	4.0	25
49	Strain stiffening, high load-invariant hardness, and electronic anomalies of boron phosphide under pressure. Physical Review B, 2020, 101, .	3.2	24
50	Microstructure, mechanical and tribological properties of Mo-V-N films by reactive magnetron sputtering. Surface and Coatings Technology, 2020, 387, 125532.	4.8	23
51	Yield strength enhancement of MgO by nanocrystals. Journal of Materials Science, 2005, 40, 5763-5766.	3.7	22
52	Kinetics of SiC formation during high P–T reaction between diamond and silicon. Diamond and Related Materials, 2005, 14, 1611-1615.	3.9	22
53	Superhard diamond/tungsten carbide nanocomposites. Applied Physics Letters, 2011, 98, .	3.3	22
54	Thermal equations of state and phase relation of PbTiO3: A high P-T synchrotron x-ray diffraction study. Journal of Applied Physics, 2011, 110, 084103.	2.5	22

#	Article	IF	CITATIONS
55	Direct observation of immiscibility in pyrope-almandine-grossular garnet. American Mineralogist, 2000, 85, 41-46.	1.9	20
56	Anisotropic elasticity of jarosite: A high-P synchrotron XRD study. American Mineralogist, 2010, 95, 19-23.	1.9	20
57	Microstructure evolution, densification behavior and mechanical properties of nano-HfB2 sintered under high pressure. Ceramics International, 2019, 45, 7885-7893.	4.8	20
58	Experimental investigation of the creep behavior of MgO at high pressures. Physics of the Earth and Planetary Interiors, 2008, 170, 170-175.	1.9	19
59	Acoustic velocities and elastic properties of pyrite (FeS2) to 9.6 GPa. Journal of Earth Science (Wuhan,) Tj ETQq1	1 0.78431 3.2	4 ₁ rgBT /Ove
60	Configuring solid-state batteries to power electric vehicles: a deliberation on technology, chemistry and energy. Chemical Communications, 2021, 57, 12587-12594.	4.1	18
61	Thermal equation-of-state of osmium: a synchrotron X-ray diffraction study. Journal of Physics and Chemistry of Solids, 2005, 66, 706-710.	4.0	17
62	In situphase transition study of nano- and coarse-grained TiO2under high pressure/temperature conditions. Journal of Physics Condensed Matter, 2008, 20, 125224.	1.8	17
63	Thermoelasticity of Â-FeSi to 8 GPa and 1273 K. American Mineralogist, 2009, 94, 1039-1044.	1.9	17
64	Comparative studies of constitutive properties of nanocrystalline and bulk iron during compressive deformation. Acta Materialia, 2011, 59, 3384-3389.	7.9	15
65	Elastic, magnetic and electronic properties of iridium phosphide Ir2P. Scientific Reports, 2016, 6, 21787.	3.3	15
66	Pressure effects on phase equilibria and solid solubility in MgO-Y2O3 nanocomposites. Journal of Applied Physics, 2012, 111, .	2.5	14
67	The relative strength of perovskite and post-perovskite NaCoF ₃ . Mineralogical Magazine, 2012, 76, 925-932.	1.4	13
68	Density and elasticity of Zr46Cu37.6Ag8.4Al8 bulk metallic glass at high pressure. Scripta Materialia, 2011, 65, 497-500.	5.2	12
69	High pressure synchrotron x-ray diffraction studies of superprotonic transitions in phosphate solid acids. Solid State Ionics, 2012, 213, 58-62.	2.7	12
70	Equations of state and phase transformation of depleted uranium DU-238 by high pressure-temperature diffraction studies. Physical Review B, 2007, 75, .	3.2	10
71	Combined in situ synchrotron X-ray diffraction and ultrasonic interferometry study of ε-FeSi at high pressure. High Pressure Research, 2008, 28, 385-395.	1.2	10
72	Compressional and shear wave velocities of Fe2SiO4 spinel at high pressure and high temperature. High Pressure Research, 2008, 28, 405-413.	1.2	10

#	Article	IF	CITATIONS
73	High-pressure phase transformations in MgO-Y2O3 nanocomposites. Applied Physics Letters, 2011, 99, .	3.3	10
74	Phase transformations in hypereutectic MgO-Y2O3 nanocomposites at 5.5 GPa. Journal of Applied Physics, 2013, 113, .	2.5	10
75	Thermal equation of state and thermodynamic Grüneisen parameter of beryllium metal. Journal of Applied Physics, 2013, 114, .	2.5	10
76	Carmichaelite, a new hydroxyl-bearing titanate from Garnet Ridge, Arizona. American Mineralogist, 2000, 85, 792-800.	1.9	9
77	Thermal equation of state of CalrO3 post-perovskite. Physics and Chemistry of Minerals, 2011, 38, 407-417.	0.8	9
78	A new lithium-rich anti-spinel in Li–O–Br system. Chemical Communications, 2015, 51, 9666-9669.	4.1	9
79	Thermal equation of state of CaGeO3 perovskite. American Mineralogist, 2008, 93, 745-750.	1.9	8
80	Thermal equation of state of TiC: A synchrotron x-ray diffraction study. Journal of Applied Physics, 2010, 107, .	2.5	8
81	In situ ultrasonic velocity measurements across the olivine-spinel transformation in Fe2SiO4. American Mineralogist, 2010, 95, 1000-1005.	1.9	8
82	Structural and Physical Properties of ZrSi2 under High Pressure: Experimental Study and First-Principles Calculations. Inorganic Chemistry, 2019, 58, 405-410.	4.0	8
83	Comparative studies of yield strength and elastic compressibility between nanocrystalline and bulk cobalt. Journal of Applied Physics, 2012, 111, .	2.5	7
84	Thermal equation of state of a natural kyanite up to 8.55 GPa and 1273 K. Matter and Radiation at Extremes, 2016, 1, 269-276.	3.9	7
85	Structural disorder, sublattice melting, and thermo-elastic properties of anti-perovskite Li3OBr under high pressure and temperature. Applied Physics Letters, 2020, 117, .	3.3	7
86	Novel Nitride Materials Synthesized at High Pressure. Crystals, 2021, 11, 614.	2.2	6
87	Density measurements of molten materials at high pressure using synchrotron X-ray radiography: melting volume of FeS. , 2005, , 185-194.		6
88	Three-dimensional visualization of lithium metal anode via low-dose cryogenic electron microscopy tomography. IScience, 2021, 24, 103418.	4.1	6
89	Concurrent Pressure-Induced Spin-State Transitions and Jahn–Teller Distortions in MnTe. Chemistry of Materials, 2022, 34, 3931-3940.	6.7	6
90	An exploratory study of the viscoelasticity of phase-transforming material. Physics of the Earth and Planetary Interiors, 2009, 174, 174-180.	1.9	4

#	ARTICLE Strain-driven structural selection and amorphization during first-order phase transitions in	IF	CITATIONS
91	nanocrystalline <mml:math xmlns:mml="http://www.w3.org/1998/Math/MathML"><mml:mrow><mml:msub><mml:mi>Ho</mml:mi><mml:n mathvariant="normal">O<mml:mn>3</mml:mn></mml:n </mml:msub></mml:mrow></mml:math 	າກ 3 2 <td>ll:man></td>	ll:man>
92	Elastic softening of peridotite due to the presence of melt phases at high pressure. Physics of the Earth and Planetary Interiors, 2008, 170, 176-180.	1.9	3
93	Observation of anomalous phonons in orthorhombic rare-earth manganites. Applied Physics Letters, 2010, 97, 262905.	3.3	3
94	High-Pressure Research at the National Synchrotron Light Source. Synchrotron Radiation News, 2010, 23, 24-30.	0.8	3
95	Equation of state and thermodynamic Grüneisen parameter of monoclinic 1,1-diamino-2,2-dinitroethylene. Journal of Physics Condensed Matter, 2016, 28, 395402.	1.8	3
96	Operation of large-volume cubic press above 8â€GPa and 2500°C with a centimeter-sized cell volume using an optimized hybrid assembly. High Pressure Research, 2021, 41, 132-141.	1.2	3
97	High-Pressure and High-Temperature Synthesis and In Situ High-Pressure Synchrotron X-ray Diffraction Study of HfSi ₂ . Inorganic Chemistry, 2021, 60, 15215-15222.	4.0	3
98	Compressibility and thermoelasticity of CrN. High Pressure Research, 2020, 40, 423-433.	1.2	2
99	Strengthening Superhard Materials by Nanostructure Engineering. Journal of Superhard Materials, 2021, 43, 307-329.	1.2	2
100	sp ² -to-sp ³ transitions in graphite during cold-compression. Physical Chemistry Chemical Physics, 2022, 24, 10561-10566.	2.8	2
101	Strength measurement of boron suboxide B6O at high pressure and temperature using in situ synchrotron X-ray diffraction. High Pressure Research, 2008, 28, 423-430.	1.2	1
102	Pressure-Induced Amorphization and Phase Transformations in \hat{I}^2 -LiAlSiO4 ChemInform, 2005, 36, no.	0.0	0